Proceedings of the ASME 2013 International Mechanical Engineering Congress and Exposition
IMECE2013
November 15-21, 2013, San Diego, California, USA

IMECE2013-63656

APPLICATION OF SLIDING SEGMENT AND ROLLING SEGMENTS DRAG FACTORS IN ROLL PHASE SPEED AND ROLL RATE CALCULATIONS

Mark William Arndt
Transportation Safety Technologies,
Inc.
Mesa, Arizona, USA

ABSTRACT

During the roll phase of a rollover crash and beginning at the point of trip, three segments have been distinguished. The segments are (1) the first airborne distance and (2, 3) distances associated with two segments in a bi-constant deceleration response. The bi-constant deceleration response was discovered in over-the-ground speed analysis of rollover crash video complemented by analysis of recorded instruments and detailed post-rollover documentation. The bi-constant deceleration response has been theorized as attributable in the first region to a sliding mechanism and transitioning in the second region to a rolling mechanism. Experimentally reported results are used in a probabilistic simulation to predict speed, roll rate and extent (time and angle). Results allow for predicting speed and roll rate in the time and displacement domain dictated by analyst's constraints and preferred statistical cutoffs. Description of the model is followed by examples of its application in actual rollovers and comparison to experiment results.

INTRODUCTION

In their 2009 SAE paper Rose and Beauchamp, "advance[d] rollover crash reconstruction techniques beyond the assumption typically made that a rolling vehicle decelerates at a constant rate" [1]. Their approach was to identify two or three regions over a vehicle's roll distance, assign discrete deceleration rates to each region and equate the overall deceleration to average deceleration. Two examples from crash tests were examined. The authors noted, "Overall, each of the suggested variable deceleration rate profiles represented a significant improvement over using a constant deceleration rate."

In 2011 Stevens and co-authors presented detailed Over-the-Ground Speed (OGS) analysis of five instrumented steer-induced rollover tests [2]. The testing included detailed documentation of crash surface marking, vehicle damage, vehicle marking, and plots of recorded onboard instrumentation. Stevens demonstrated a consistent bi-linear response in OGS as a function of time and noted changes in the recorded roll rate responses corresponding to the transition time of deceleration rate. The bi-linear response could also be called a bi-constant drag factor where the first phase of the roll has a higher constant drag factor compared to the second phase.

A unified model for roll motion developed and demonstrated by Funk and co-authors in 2012, described a bi-constant approach over the roll distance [3]. Funk's approach identified three distinct segments in a roll phase. Funk described a brief initial airborne phase, followed by an early phase in which the average vehicle deceleration is higher and governed by sliding friction and a final phase in which the average vehicle deceleration is lower and governed by geometric factors.

The first airborne segment of a roll phase was noted by Asay and Woolley in 2010 [4] and Stevens [2] in 2011. The importance of considering the first airborne segment in the analysis of rollover motions was demonstrated by both Funk [3] and Arndt [5] in 2012. Including the first airborne segment improved prediction of the shape of the roll and displacement

rate curves. The first airborne segment is the distance between the point of trip and the first post-trip ground contact and importantly has a characteristic of constant OGS and angular rates.

NOMENCLATURE

CDF - Constant Drag factor.

First Airborne Segment - The distance between the point of trip and the first post-trip ground contact.

OAW – Over-All Width

OAH – Over-All Height

OGS - Over-The-Ground Speed.

Rolling Distance - The distance from first post-trip ground contact to the point of rest - the sliding segment plus the rolling segment.

Roll Phase - Point of trip to the point of rest - The first airborne segment plus the sliding segment plus the rolling segment.

Rolling Segment - The second segment of the rolling distance in which an effective circumferential speed aligned with the vehicle path and parallel to the ground is equal to the translational speed of the vehicle CG.

Sliding Segment - The first segment of the rolling distance in which an effective circumferential speed aligned with the vehicle path and parallel to the ground is less than the translational speed of the vehicle CG.

METHOD

Consistent with recent approaches [1, 3, 5], the analysis predicts the translational motion of the vehicle's center of gravity and the rotation of the vehicle about its roll axis. Funk noted, "All motion is assumed to occur in the plane perpendicular to the longitudinal axis of the vehicle. Pitch, yaw, longitudinal motion, vertical motion, and impacts to the vehicle are all neglected [3]."

In the equations that follow, parameters with a 0 subscript indicate values at the point of trip or roll phase initiation (end of tire marks). Point of trip is the zero point for time and distance and denotes the beginning of the first airborne segment. Parameters with a 1 subscript denote values at the beginning of the rollover's sliding segment. Parameters with a 2 subscript denote values at the time of the beginning of the rolling segment. Final values at the end of the rolling are denoted by a f subscript. The sliding and rolling segments are denoted with a s and r subscript, respectively.

The constitutive equations start with the approach of Rose and Beauchamp [1] in which the speed at the point of trip, S_0, was calculated from a Constant Drag Factor (CDF) and the roll phase distance, d_f (Equation 1). Speed at the point of trip, S_0, is equal to the speed at first ground contact, S_1 (Equation 2). The roll phase distance, d_f, and distance of the first airborne segment, d_1, are provided by the analyst. Using a traditional conservation of energy approach the speed at the point of sliding segment to rolling segment transition, S_2, is then calculated (Equation 3). The fraction of sliding segment distance to rolling distance is denoted by $\%_S$. The final speed, s_f, is zero.

(1) $S_0 = \sqrt{2 \times g \times CDF \times d_f}$, (ft/s)

(2) $S_0 = S_1$, (ft/s)

(3) $S_2 = \sqrt{2 \times g \times f_r \times (1 - \%_S) \times (d_f - d_1)}$, (ft/s)

The time at each roll phase segment position was calculated:

(4) $t_1 = d_1/S_0$, (s)

(5) $t_2 = t_1 + (S_2 - S_1)/(g \times f_s)$, (s)

(6) $t_f = t_2 + S_2/(g \times f_r)$, (s)

The Funk model, with its bi-constant approach, dictates that the peak roll rate occurs at the transition from the sliding segment to the rolling segment and that in the rolling segment the vehicle center of gravity (CG) is positioned directly above its ground contact [3]. From the Funk assumptions, the peak roll rate, ω_2, was calculated by equation 7 assuming an effective radius, r_{eff}, dictated by vehicle geometry, equation 8. The roll rate with analyst input for α_0 and α_1 was calculated for the first airborne phase from equation 9.

(7) $\omega_2 = S_2/r_{eff}$, (rad/s; deg/s = $180/\pi$ (rad/s)

(8) $r_{eff} = (OAW + OAH)/\pi$, (ft)

(9) $\omega_0 = \omega_1 = (\alpha_1 - \alpha_2)/t_1$, (rad/s or degree/s)

Prediction of a distribution of roll motions used a Monte Carlo method in a Microsoft Excel spreadsheet to propagate the uncertainty in the probabilistic simulation. The use of Excel spreadsheets in performing Monte Carlo analysis was described by Bartlett in his 2003 SAE Paper, Conducting Monte Carlo Analysis with Spread Sheet Programs [6]. According to Bartlett, a Monte Carlo analysis evaluates the constitutive equations of an analysis many times, each time selecting the variable values based on their specified probability. The series of trials generates a group of possible results (a sample). A

TestID	units	O5	O6	T6	S0	S1	S2	S3	S4	A1	A2	A8	AN	Avg (all)	SD (all)
f_1	(g)	-0.48	-0.85	-0.89	-0.54	-0.82	-0.61	-0.63	-0.8	-1.43	-1.05	-1.48	-0.54	-0.84	0.33
f_2	(g)	-0.31	-0.35	-0.22	-0.21	-0.22	-0.27	-0.27	-0.4	-0.26	-0.29	-0.27	-0.23	-0.27	0.06
d_1	(ft)	3	9	3	11	22	15	11	14	35	28	34	22	17	11
d_2	(ft)	39	38	23	67	119	76	35	71	69	61	69	169	70	40
d_f	(ft)	90	65	69	106	265	147	93	105	266	184	234	249	156	79
d_2/d_f	(%)	44%	59%	33%	64%	45%	52%	38%	67%	26%	33%	29%	68%	46%	15%
$(d_2-d_1)/(d_f-d_1)$	(%)	41%	52%	30%	59%	40%	46%	29%	63%	15%	21%	18%	65%	40%	18%

Table 1. Selected data from Funk [3] used in the probabilistic simulation, including values for $(d_2-d_1)/(d_f-d_1)$.

	Test #	df (ft)	d1 (ft)	OAH (in)	OAW (in)	# rolls (count)
2001 2DR 2WD Chevroley Blazer	S1	264.7	22.4	66	68	9
2002 2WD Ford Explorer Sport	S2	146.7	14.9	68	70	5
1997 4WD Ford Explorer Sport	S3	92.4	11.1	68	70	3 1/2
1995 4WD Nissan Pathfinder LE	S4	105.2	13.9	66	67	3

Table 2. Data from the four (4) steer induced rollover tests used in comparison to the predicted rollover response, from Stevens [2].

range of the results that fall into selected intervals about the median is lower than what would be generated by a simple worst-or-best case approach [6].

Table 1 summarizes data from selected rows of the Funk paper that were used in the probabilistic simulation [3]. In addition, Table 1 includes the row calculating $(d_2-d_1)/(d_f-d_1)$. Because the standard deviation of $(d_2-d_1)/(d_f-d_1)$ was large, the distribution for this parameter is trimmed utilizing the range of the minimum and maximum calculated values of 15% to 65%. The CDF was a 0.44 g average (SD = 0.064 g) from analysis presented in a 2011 ASME paper analyzing 81 dolly rollover tests and 24 steer-induced rollover tests [7].

Table 2 summarizes reconstruction data from the four steer-induced rollover tests used in comparison to the predicted rollover response. The steer-induced rollover tests were presented by Stevens in his 2011 SAE technical paper [2] and are included in the 24 steer-induced rollover tests previously described [7]. Table 2 includes dimensions for the Over-All Height (OAH) and Over-All Width (OAW). Because the instrument failed to record during the test, the roll rate for test 4 was calculated by Funk through video analysis. Funk presented the calculated roll rate of test 4 in his 2012 SAE paper [3].

RESULTS

Figure 1 through Figure 4 are in Annex A and compare measured roll rate and calculated OGS results from test one through four as presented in Stevens' 2011 paper, respectively, to the probabilistic analysis derived speed and roll rate. Comparison results are upper and lower referring, respectively, to plus and minus one standard deviation from the calculated distribution's average result. Table 3 summarizes the calculated and actual roll duration. The roll duration in the testing was defined to have ended when the vehicle first rolls to its final rest position. If the vehicle overshot the final rest position and then rocked back to final rest, the time representing the overshoot was neglected. Table 4 and Table 5 summarize the calculated and actual maximum roll rate and time of maximum roll rate, respectively. Actual roll rates are from recorded test data filtered to SAE class 60.

Test No.	Roll Phase Duration (sec)			
	From Assumed Drag Factor			Actual
	average	upper	lower	
S1	7.56	8.36	6.75	7.58
S2	5.56	6.17	4.95	5.31
S3	4.42	4.87	3.96	3.70
S4	4.74	5.25	4.23	3.58

Table 3. Calculated and actual roll duration.

DISCUSSION

The probabilistic analysis of each rollover using a bi-constant drag factor and Funk's unifying theory predicted a corridor of rollover speed and roll rate response versus time that mostly encompassed the actual response of the four comparison steer-induced rollovers. The predictions' agreement was partially caused because the rollovers were a

Test No.	Roll rate Peak (deg/sec)			
	From Assumed Drag Factor			Actual
	average	upper	lower	
S1	799	881	717	757
S2	534	589	479	734
S3	446	495	398	580
S4	395	440	350	415*
*based upon video analysis only				

Table 4. Calculated and actual maximum roll rate and time of maximum roll rate.

Test No.	Time of Roll Rate Peak (sec)			
	From Assumed Drag Factor			Actual
	average	upper	lower	
S1	1.95	2.09	1.80	1.84
S2	1.76	1.91	1.62	1.69
S3	1.27	1.41	1.13	0.71
S4	1.70	1.58	1.81	1.50*
*based upon video analysis only, last peak calculation				

Table 5. Calculated and actual time of maximum roll rate.

subset of the population used in the derivation of the models input variables. The model's inputs appeared to consistently predict a response corridor that missed portions of the rate of roll rate onset during the sliding phase of the response.

A notable difference was observed in the over prediction of the roll rate of test S1. Test S1 had the greatest number of rolls and the highest speed. At the opposite end of the rollover test distribution, test S3 tripped at the lowest speed and the peak roll rate was under predicted. A cause of test S3's roll rate under prediction was that the actual CDF was less than one standard deviation of the modeled average CDF. The roll duration in test S4 was longer than modeled. Test S4's CDF was greater than one standard deviation of the modeled average CDF. A mechanism for arresting the roll in test S4 involved the release of the vehicle's rear spare tie mount. The vehicle in test S4 was not purely rolling at the end of its rolling phase because the spare tire mount effectively acted as an outrigger helping to bring the vehicle to a stop.

A key factor in predicting the roll rate time history is choosing a deceleration model that properly predicts the total rollover duration. The probabilistic analysis predicted a roll duration corridor that encompassed the actual roll duration in all tests except S4. A model that tends to underestimate the rollover duration (typical of a constant deceleration method and high average deceleration in a LVDR method) will overestimate the roll rate. Conversely, a model that overestimates the rollover duration will underestimate roll rates.

CONCLUSION

Probabilistic analysis using the bi-constant roll response and the unifying theory described by Funk can be used to predict specific aspects of a vehicle's rollover response in situations when minimal information from the scene of a rollover is available. Likewise the method provides the opportunity for the calculation of details in the rollover response in retrospective analysis of rollover crashes that have only the most basic information regarding speed or roll distance. The model can only be expected to accurately predict rollover motion when an analyst can confirm that no unusual roll events occurred and the scene and vehicle damage are consistent with sliding and rolling motions.

REFERENCES

(1) Rose, N. A. and Beauchamp, G., "Development of a Variable Deceleration Rate Approach to Rollover Crash Reconstruction," SAE Technical Paper 2009-01-0093, 2009, doi: 10.4271/2009-01-0093.

(2) Stevens, D. C., Arndt, S. M., Wayne, L., Arndt, M. W., Anderson, R., Manning, J., et al., "Rollover Crash Test Results: Steer-Induced Rollovers," SAE Technical Paper 2011-01-1114, 2011, doi:10.4271/2011-01-1114.

(3) Funk, J., Wirth, J., Bonugli, E., Watson, R., Asay, A. F., "An Integrated Model of Rolling and Sliding in Rollover Crashes," SAE Technical Paper 2012-01-0605, 2012, doi: 10.4271/2012-01-0605.

(4) Asay, A. F. and Woolley, R. L., "Rollover Testing of Sport Utility Vehicles (SUVs) on an Actual Highway'" SAE Technical Paper 2010-01-0521, 2010, doi:10.4271/2010-01-0521.

(5) Arndt, M. W., Stevens, D., Arndt, S. M., "Comparison of Linear Variable Deceleration Rate Rollover Reconstruction to Steer-Induced Rollover Tests," SAE Technical Paper 2012-01-0469, 2012, doi:10.4271/2012-01-0469.

(6) Bartlett, W., "Conducting Monte Carlo Analysis with Spread Sheet Programs," SAE Technical Paper 2003-01-0487, 2003, doi:10.4271/2003-01-0487.

(7) Arndt, M. W., Arndt, S. M., Stevens, D., "Drag Factors from Rollover Crash Testing for Crash Reconstructions," Paper IMECE2011-65537 presented at ASME International Mechanical Engineering Congress and Exposition, 2011, doi:10.1115/*IMECE2011-65537*.

CONTACT INFORMATION

Mark W. Arndt, PO BOX 30717, Mesa, AZ 85275
marndt@transport-safety.com, 602-432-8515

ANNEX A

FIGURES 1 THROUGH 4, SHOWING THE MEASURED VS. PREDICTED RESPONSE OF OGS AND ROLL RATE

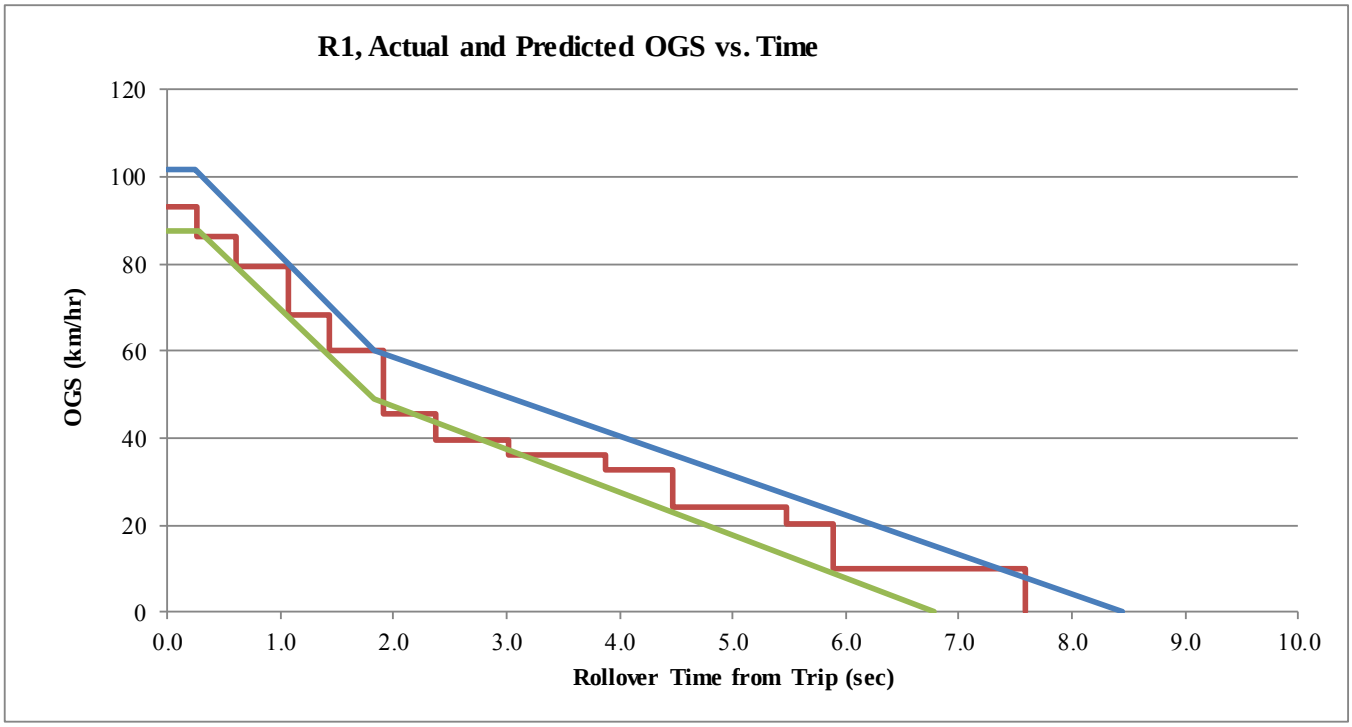

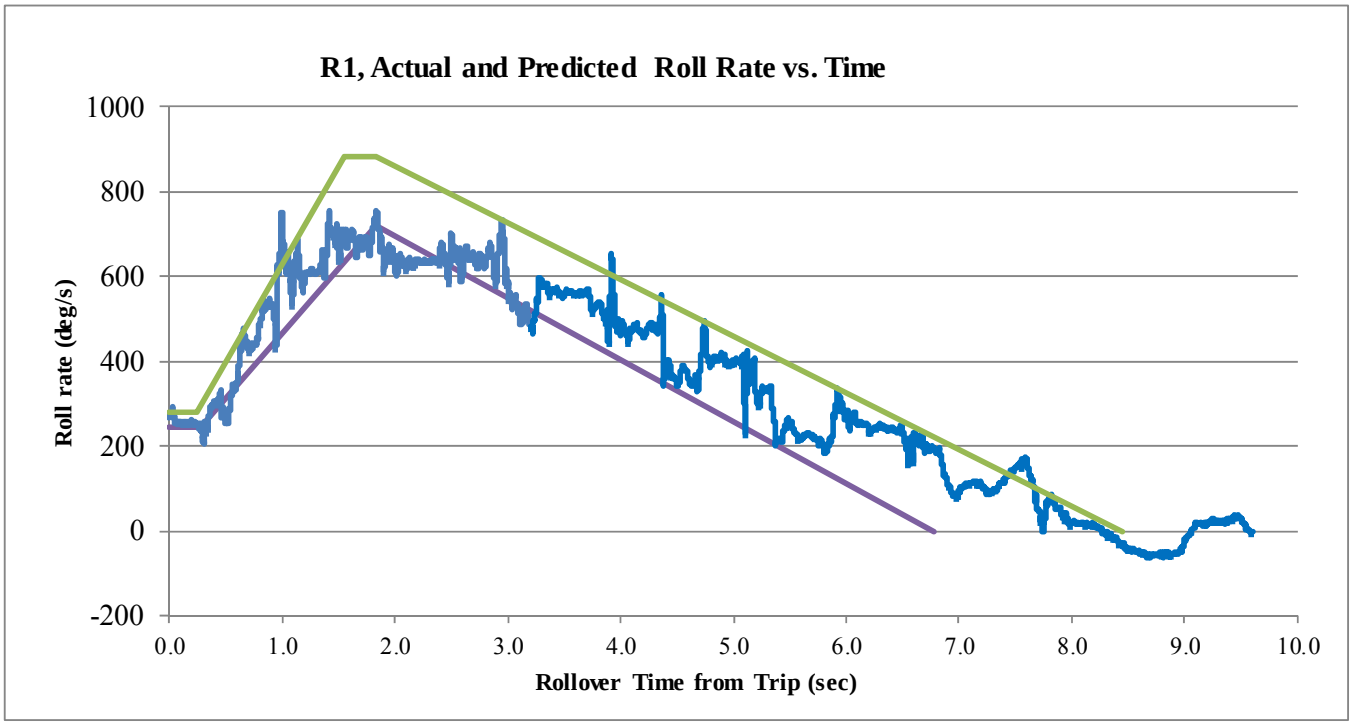

Figure 1. Predicted OGS and roll rate responses compared to Stevens' test R1 [2].

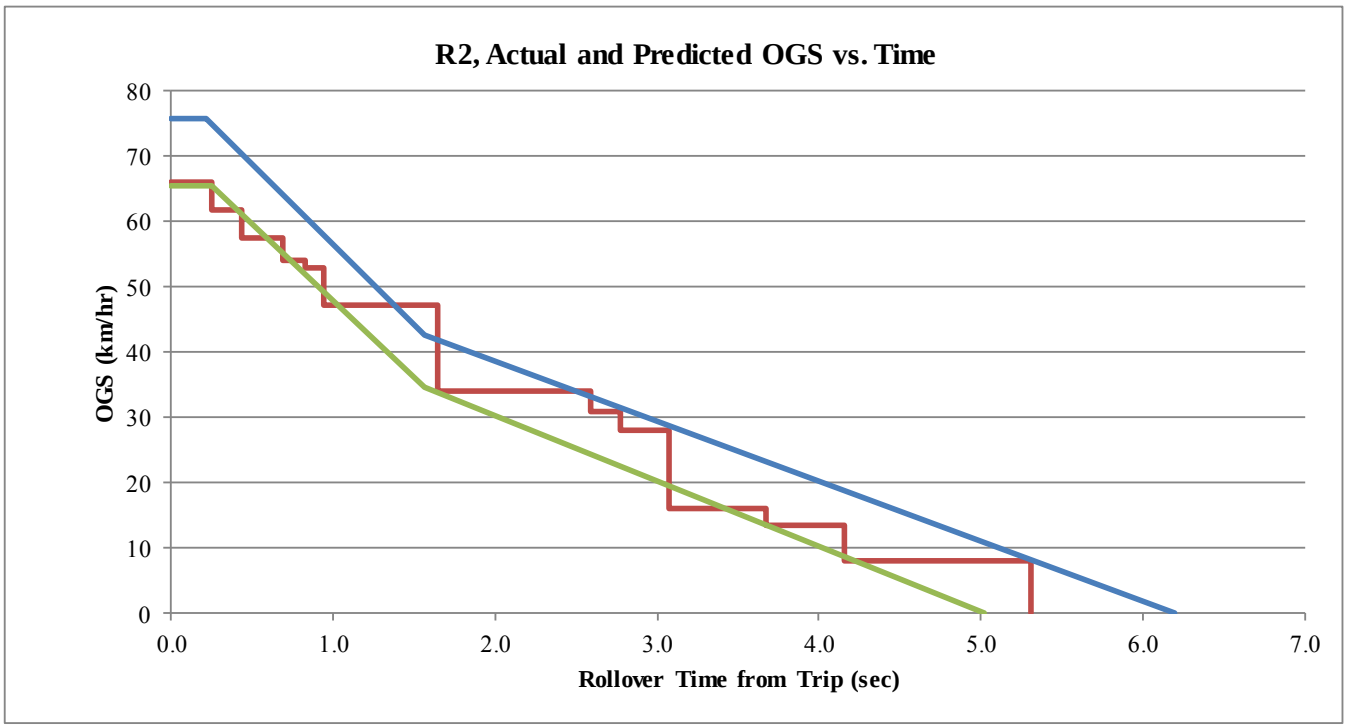

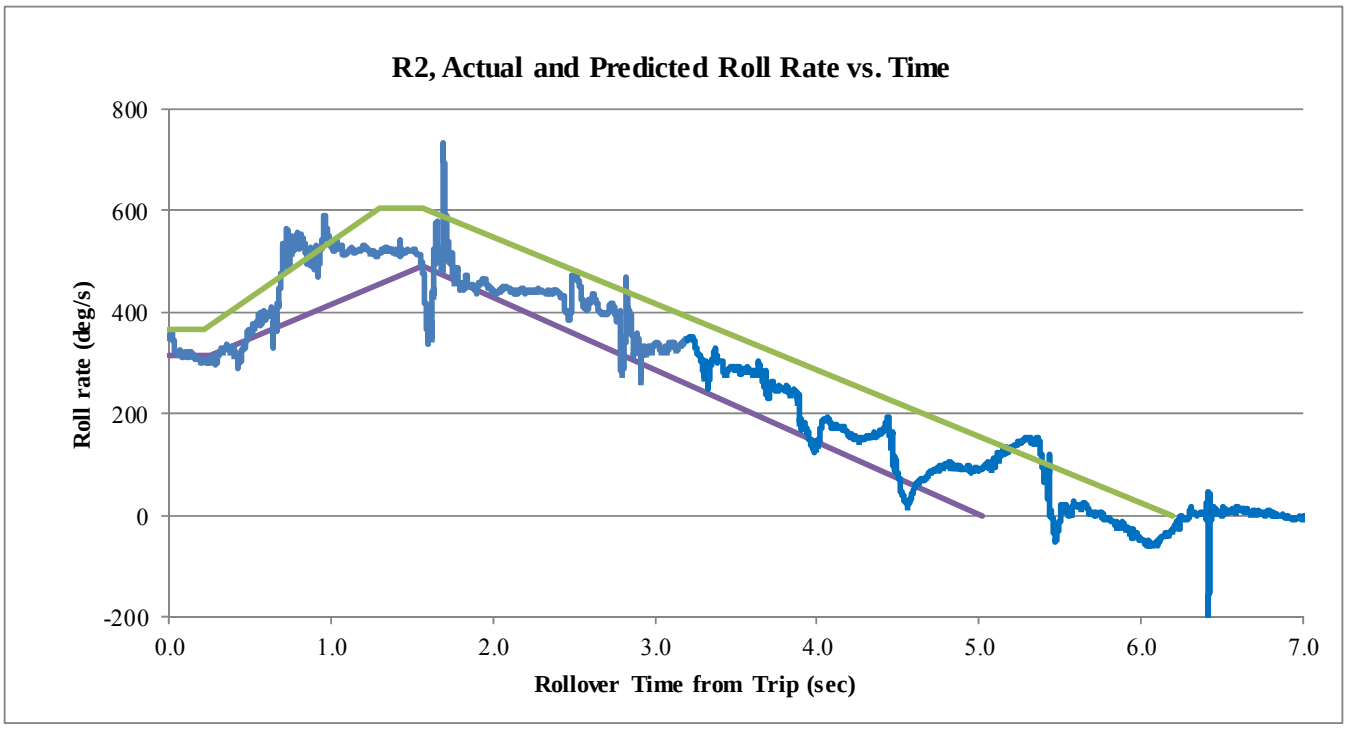

Figure 2. Predicted OGS and roll rate responses compared to Stevens' test R2 [2].

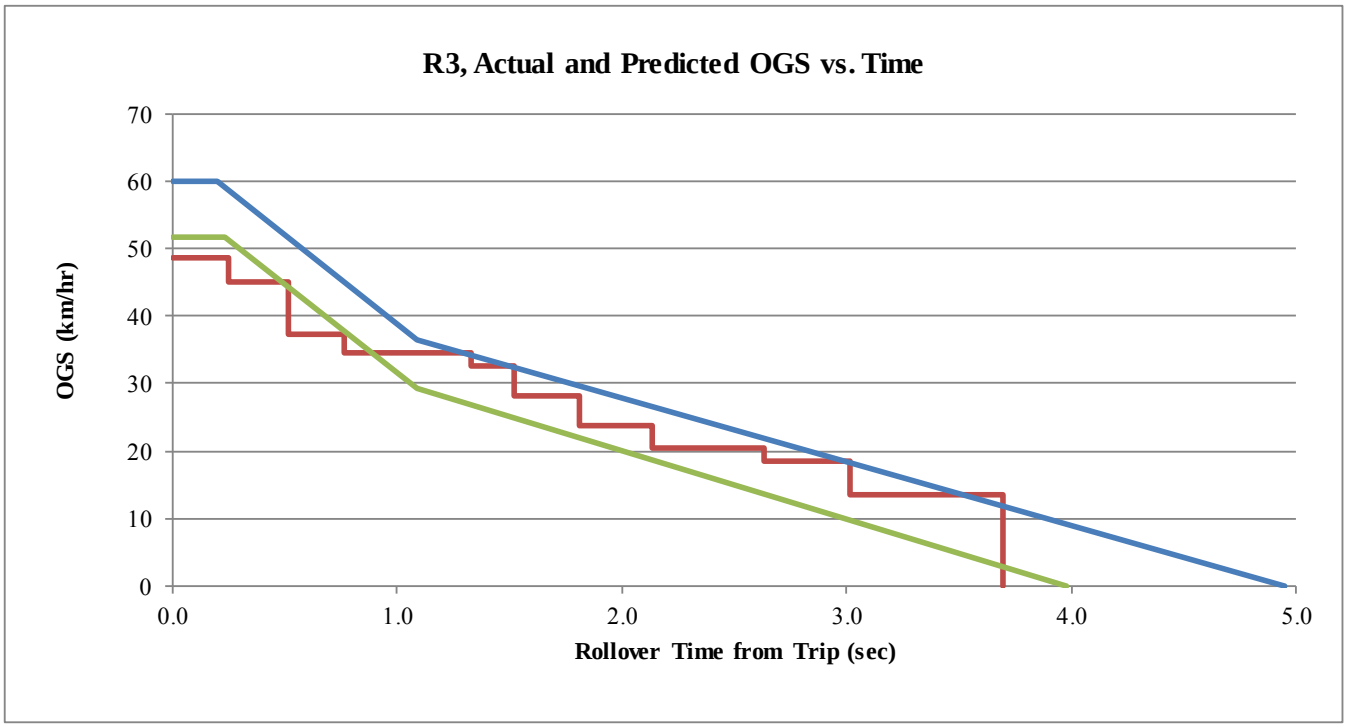

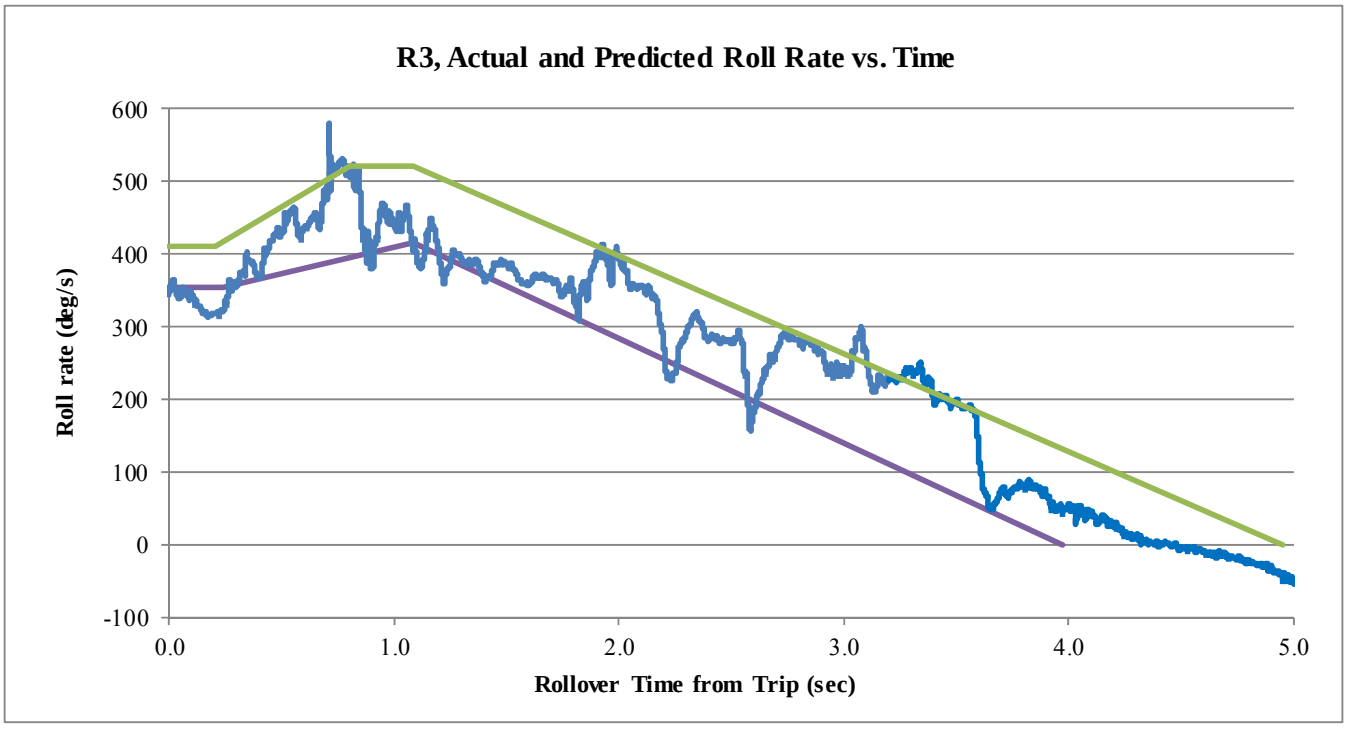

Figure 3. Predicted OGS and roll rate responses compared to Stevens' test R3 [2].

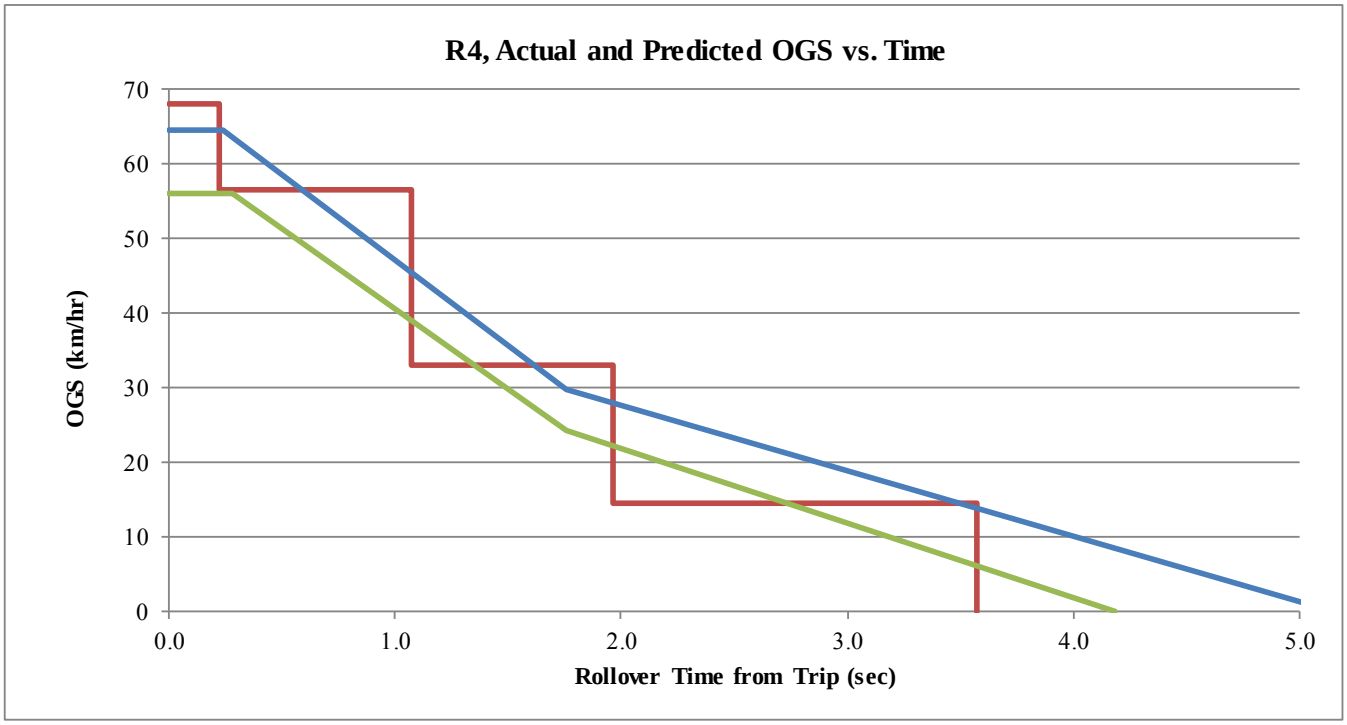

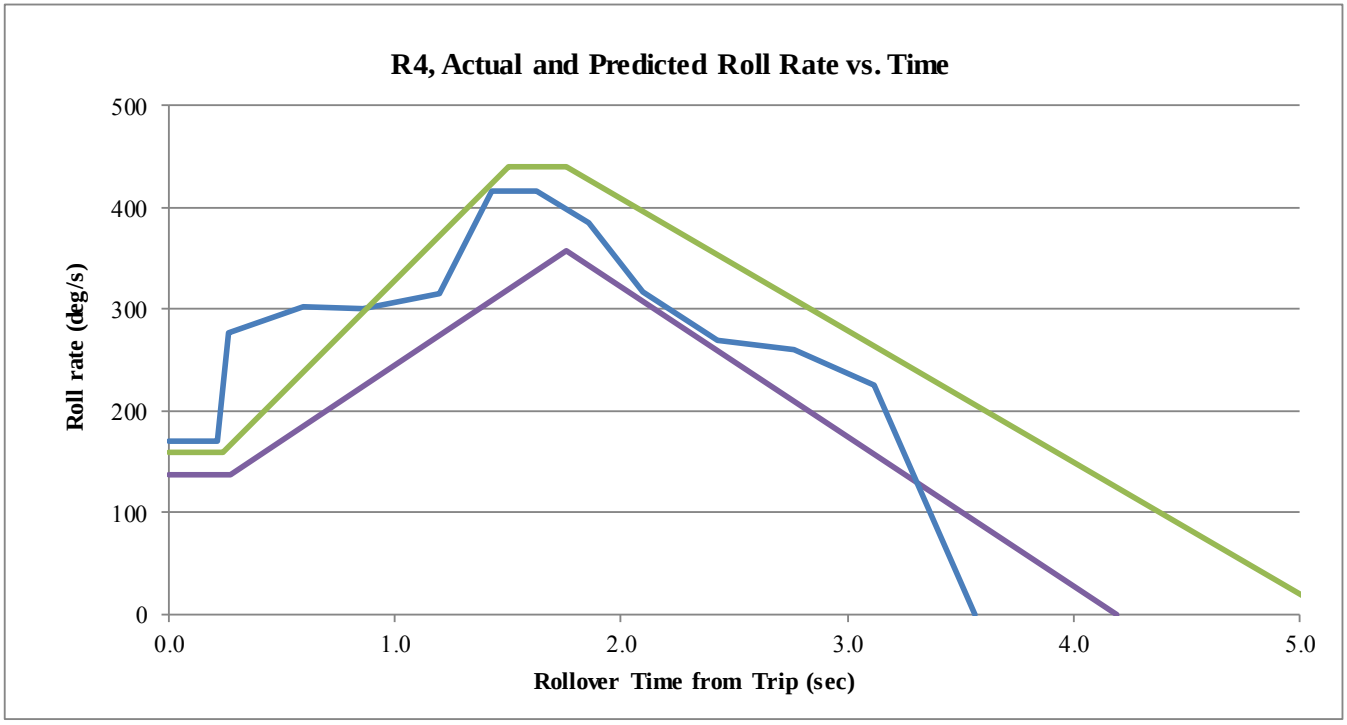

Figure 4. Predicted OGS and roll rate responses compared to Stevens' test R4 [2].